Enzyme catalytic amplification of miRNA-155 detection with graphene quantum dot-based electrochemical biosensor

Tianxing Hu, Le Zhang, Wei Wen, Xiuhua Zhang, Shengfu Wang

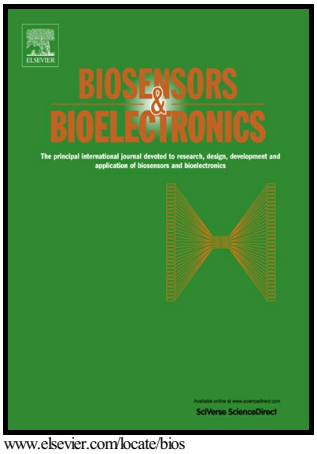

www.elsevier.com/locate/bios

PII: S0956-5663(15)30464-4
DOI: http://dx.doi.org/10.1016/j.bios.2015.09.068
Reference: BIOS8035

To appear in: *Biosensors and Bioelectronic*

Received date: 5 August 2015
Revised date: 18 September 2015
Accepted date: 29 September 2015

Cite this article as: Tianxing Hu, Le Zhang, Wei Wen, Xiuhua Zhang and Shengfu Wang, Enzyme catalytic amplification of miRNA-155 detection witl graphene quantum dot-based electrochemical biosensor, *Biosensors an Bioelectronic,* http://dx.doi.org/10.1016/j.bios.2015.09.068

Enzyme catalytic amplification of miRNA-155 detection with graphene quantum dot-based electrochemical biosensor

Tianxing Hu, Le Zhang, Wei Wen*, Xiuhua Zhang, Shengfu Wang*

Hubei Collaborative Innovation Center for Advanced Organic Chemical Materials, Ministry of Education Key Laboratory for the Synthesis and Application of Organic Functional Molecules & College of Chemistry and Chemical Engineering, Hubei University, Wuhan 430062, PR China

*Corresponding author.

Telephone: +86-27-50865309; Fax: +86-27-88663043; E-mail address: wenwei@hubu.edu.cn; wangsf@hubu.edu.cn.

Abstract

A specific and sensitive method was developed for quantitative detection of miRNA by integrating horseradish peroxidase (HRP)-assisted catalytic reaction with a simple electrochemical RNA biosensor. The electrochemical biosensor was constructed by a double-stranded DNA structure. The structure was formed by the hybridization of thiol-tethered oligodeoxynucleotide probes (capture DNA), assembled on the gold electrode surface, with target DNA and aminated indicator probe (NH_2-DNA). After the construction of the double-stranded DNA structure, the activated carboxyl groups of graphene quantum dots (GQDs) assembled on NH_2-DNA. GQDs were used as a new platform for HRP immobilization through noncovalent assembly. HRP modified biosensor can effectively catalyze the hydrogen peroxide (H_2O_2)-mediated oxidation of 3,3′,5,5′-tetramethylbenzidine (TMB), accompanied by a change from colorless to blue in solution color and an increased electrochemical current signal. Due to GQDs and enzyme catalysis, the proposed biosensor could sensitively detect miRNA-155 from 1 fM to 100 pM with a detection limit of 0.14 fM. High performance of the biosensor is attributed to the large surface-to-volume ratio, excellent compatibility of GQDs. For these advantages, the proposed method holds great potential for analysis of other interesting tumour makers.

Keywords

Graphene quantum dots; Electrochemical biosensor; miRNA-155; Horseradish peroxidase

1. Introduction

MicroRNAs (miRNAs) are a class of noncoding RNA molecules with a length of 17-25 nucleotides that function in RNA silencing and post-transcriptional regulation of gene expression (Qiu et al. 2015), playing critical regulatory functions in many biological processes such as tumorigenesis, metastasis, diagnosis, prognosis, cell differentiation, cell apoptosis and protein synthesis (Lu et al. 2005; Jiang et al. 2015; Lewis et al. 2003; Mitchell et al. 2008; Lim et al. 2005). Studies on functions of miRNA proved that it could be an oncogene or a tumor suppressor gene. miRNA-155 targeting oncogenes could act as a tumor suppressor, whereas targeting tumor suppressor genes could be a potential oncogene (Wang et al. 2012; Wei et al. 2013). At the same time, the expression and functions of miRNAs were regulated by various factors, such as gene sequence, phosphorylation level, miRNAs modification enzyme, etc (O'Connell et al. 2007), these observations identify a potential link between inflammation and cancer. Therefore, miRNAs have become clinically important biomakers for early cancer diagnostic and prognostic processes (Pritchard et al. 2012; Wen et al. 2012; Yang et al. 2012; Duan et al. 2013). miRNA-155 expression during myocarditis was localized primarily in infiltrating macrophages and T lymphocytes (Duan et al. 2013). Corsten’s data show that cardiac microRNA dysregulation is a characteristic of both human and mouse viral myocarditis. The inflammatory microRNA-155 is upregulated during acute myocarditis, contributes to the adverse inflammatory response to viral infection of the heart, and is a potential therapeutic target for viral myocarditis (Corsten et al. 2012). Beyond the acute phase, microRNA-155 inhibition reduced mortality and improved cardiac function during 7 weeks of follow-up.

Thus, sensitive and selective detection of miRNAs is of significance in assessing the prognosis and monitoring the response to treatment. Until now, various analytical methods, such as

electrochemistry (Cheng et al. 2015; Ge et al. 2014), fluorescent (Causa et al. 2015), electrochemiluminescence (ECL) (Zhang et al. 2015; Hao et al. 2014), surface plasmon resonance (Ding et al. 2015), colorimetric analysis (Zhang et al. 2009), have been implemented to achieve sensitive detection of miRNA. Among these methods, electrochemical methods have attracted considerable attention for miRNA detection for its easy controllability, good stability, acceptable reproducibility, high sensitive and low cost.

Graphene is a two dimensional honeycomb network of sp^2 hybridized carbon atoms having unique electrical, optical and structural properties. It is being vastly studied for applications in analytical, bioimaging, catalysis and photovoltaic devices (Zhu et al. 2010; Liu et al. 2012; Xiang et al. 2012). Much efforts have been made to convert the 2D graphene sheets into 0D graphene quantum dots (Gupta et al. 2011; Lin and Zhang 2012; Li et al. 2012; Li et al. 2013). GQDs are single or few-layer graphenes with a tiny size of only several nanometers (Cheng et al. 2012), they possess some excellent characteristics, such as chemical stability, excellent water solubility and suitability (Zhu et al. 2012). GQDs possess a larger number of carboxyl groups, much smaller volumes than graphene, and have a good electrical conductivity (Wang et al. 2015). Importantly, the carboxylic acid moieties at the edge of GQDs makes it easy to functionalise with various organic, polymeric, inorganic or biological species (Baker and Baker 2010). Based on the formation of an amide bond between a carboxyl group and an amino group (Wang et al. 2013), we have proposed the development of a sensitive RNA biosensor by interacting GQDs with single stranded amino-terminated DNAs.

Herein, a sensitive electrochemical RNA biosensor based on GQDs and HRP is fabricated for the detection of miRNA-155. GQDs with good biocompatibility, suitable conductivity, low toxicity were employed as the carrier for enzyme immobilization. Due to the large surface-to-volume ratio, excellent

compatibility of GQDs, large amount of HRP immobilized on GQDs through noncovalent assembly (He et al. 2014), providing high electrochemical reduction signals. Therefore, the proposed biosensor exhibited good sensitivety and selectivity with a low detection limit of 0.14 fM and could meet the requirements for direct detection of miRNA-155 in human serum, showing great potential in clinical detection.

Please, insert Fig. 1 here.

2. Experimental sections

2.1. Reagents and materials

GQDs were purchased from XFNANO Materials Tech Co.,Ltd (Nanjing, China). HRP was purchased from Aladdin Industrial Corporation 16050 (USA). Tris (2-carboxyethyl) phosphine hydrochloride (TCEP) and 6-mercapto-1-hexanol (MCH) were purchased from Sigma-Aldrich (USA). N-(3-(dimethylaminopropyl)-N'-ethylcarbodiimide hydrochloride (EDC), N-hydroxysuccinimide (NHS), 30% H_2O_2 and 3,3′,5,5′-tetramethylbenzidine (TMB) were purchased from Aladdin Reagent Company (Shanghai, China). All other reagents were of analytical grade. In our work, 10mM phosphate buffered saline (PBS pH 7.4) was used as supporting electrolyte, and 20 mM Tris-HCl (pH 7.4) containing 140 mM NaCl, 5 mM Mg^{2+} was used to prepare an aptamer solution. All aqueous solutions were prepared with ultrapure water (18.25 MΩ·cm) produced by an Aquapro water purification system.

Oligonucleotides were obtained from Sangon Biotech Co., Ltd (Shanghai, China). The sequences of these oligonucleotides were as follows:

Capture DNA: 5'-HS-$(CH_2)_6$-TTTTTTATCACGA-3'

miRNA-155: 5'-UUAAUGCUAAUCGUGAUAGGGG-3'

miRNA-21: 5'-UAGCUUAUCAGACUGAUGUUGA-3'

Non-complementary DNA (DNA): 5'-ACTGCATGAGATTTTCCACAT-3'

NH_2-DNA: 5'-TTAGCATTAATTTT-NH_2-3'

2.2. Apparatus

All electrochemical measurements were carried out with a CHI 660E electrochemical work station (Chenhua, Shanghai) using a conventional three-electrode system that consisted of a platinum wire auxiliary electrode, a saturated calomel reference electrode (SCE) and a 2-mm diameter gold working electrode (GE). Caution: the saturated calomel reference electrode is fragile and should be handled with extreme caution when it broke. All electrochemical characterizations including cyclic voltammetry (CV) and electrochemical impedance spectroscopic (EIS) measurements were conducted. CV was carried out at a scan rate of 50 mV/s. Amperometric detection was fixed at 150 mV, and the electrochemical reduction current was measured 100 s after the HRP redox reaction reached steady state.

2.3. Preparation of electrochemical biosensor

The GE was polished carefully with 0.05 μm alumina slurries, followed by sequential sonication in distilled water and ethanol for 5 min each to remove residual alumina powder. Cyclic voltammetry of 0.5 M H_2SO_4 was then repeated ten times at a scan rate of 100 mV/s between −0.2 and 1.6 V until reproducible voltammetric peaks were obtained. After rinsed thoroughly with doubly distilled water and dried with nitrogen stream, the well-cleaned electrode was immediately used for capture strand immobilization.

The well-cleaned electrode was next incubated in 1 μM capture DNA containing 0.2 mM TCEP for 12 h at room temperature, followed by rinsing with doubly distilled water. TCEP is an effective disulfide bond reducing agent. It was used to cut off disulfide bond, preventing the capture DNA from

crosslinking, which ensure more capture DNA fixing onto GE. Then, the capture DNA-modified electrode was immersed in 1 mM MCH for 1 h. MCH plays three key roles in the experiment. First, it displaces weakly bound DNA strands from the surface, while chemically attached strands by thiol linker remain tethered to the Au surface. Second, MCH forms a dense sublayer which detaches the backbones of the linked DNA strands from the surface, and provides sufficient space between probes for hybridization since the short carbon chain of MCH will not interfere with the hybridization reaction. Third, MCH also prevents unspecific adsorptions of target RNA, NH_2-DNA and HRP to the gold substrate through hydrophobic and electrostatic interaction (Tang et al. 2009). Finally, it was rinsed with pH 7.4 PBS to remove physically adsorbed DNA and MCH. After rinsed with PBS, the electrode was incubated with a mixture solution containing 25 μL miRNA-155 with different concentrations and 25 μL 1 μM NH_2-DNA for 2 h at 37 ℃ to perform the hybridization reaction. First, part of the target RNA hybridized with capture DNA through DNA base-pairing interactions, then NH_2-DNA hybridized with another part of RNA similarly. Next, the electrode immersed in a GQD solution containing EDC (400 mM) and NHS (100 mM) for 2 h. The characterization of GQDs is shown in Fig. S1. Fig. S1 indicates that the diameters of the as-prepared GQDs are in the range of 5-15 nm. The EDC and NHS solutions were used to activate the carboxyl groups of GQDs. After that, a desired quantity of HRP was allowed to attach to the electrode. Electrochemical behaviors of the step by step surface modification of the biosensor were investigated by EIS and CV.

3. Results and discussion

3.1 Principle of the electrochemical biosensor

This electrochemical biosensor for miRNA detection involves enzyme catalysis and GQDs as a new platform for immobilization. As shown in Fig. 1, in the absence of miRNA-155, capture DNA

could not hybridize with NH_2-DNA, the biosensor could not be constructed. Hydrogen peroxide oxided slowly, resulting a low signal. In the presence of miRNA-155, part of target RNA hybridized with capture DNA, then NH_2-DNA hybridized with another part of RNA. In this way, the double-stranded DNA structure was constructed. Then the activated carboxyl group of GQDs reacted with the amino of NH_2-DNA by amide bond. After that, HRP was noncovalently bound to the surface of GQDs. In the presence of the HRP, H_2O_2 converts the colorless TMB to a free radical with a single electron and the free radicals further polymerized into the blue derivative oxTMB (Liu et al. 2015), resulting in the increased signal. To quantify the electroreduction current of TMB, we use the i-t curve to measure the current from the electrocatalytic reaction. The significantly increased current was measured in a certain volume of working solution of 10 mM PBS (pH 7.4) containing 1.0 mM H_2O_2 and 15 μL of 15 mM TMB. The relatively large difference makes our detection sensitive.

3.2 Characterization of biosensor fabrication

The biosensor was characterized by electrochemical EIS and CV measurements. EIS can provide more prolific information about the interface property change of the DNA modified electrode, since the increase in semicircle diameter of EIS spectrum is equal to the increase of the interfacial electrons transfer resistance (R_{et}). Fig S2A shows the Nyquist plots of the EIS obtained in 0.5 mM $Fe(CN)_6^{3-/4-}$ solution containing 0.1 M KCl at different electrodes. The frequency range was between 0.02 Hz and 10 kHz. Bare electrode exhibited an almost straight line (curve a), the straight line corresponds to Warburg diffusion impedance, and that no semicircle observed here indicates negligible electron transfer resistance and hence a fast electron transfer. After thiolated capture DNA self-assembled onto the electrode surface, the R_{et} increased significantly by 60-fold (curve b), compared to bare electrode, because the oligonucleotides were non-conductive. After blocked by MCH, the R_{et} further increased by

150% (curve c). When the GE immersed in 1 μM NH_2-DNA and 1 pM target RNA, the R_{et} was further increased (curve d) due to the steric hindrance of electron transfer after target RNA hybridized with capture DNA and NH_2-DNA. These results were in a good agreement with those obtained from CV measurements (Fig. S2B). The bare GE exhibited a well-defined redox peak of $Fe(CN)_6^{3-/4-}$ (curve a). When capture DNA assembled on the GE, the CV peak current decrease due to the increase of R_{et} (curve b). After MCH blocked the modified electrode, the peak current decreased (curve c). Additionally, the peak current decreased after target RNA hybridized with capture DNA and NH_2-DNA (curve d).

3.3 Catalytic performance of HRP

To investigate the catalytic effect of HRP, the performance of the proposed biosensor in the absence and presence of HRP were compared. As shown in Fig. 2, in the absence of target RNA and HRP, electrochemical reaction will not be catalyzed, then it presented a low signal (18.6 nA) (curve a). In the absence of HRP, we obtain a current of 840 nA (curve c) when we detection the target RNA of 1 pM, which is 29 times higher than the current (28.9 nA) (curve b) without HRP. Because HRP amplified the final electrochemical signal through the catalytic reaction of H_2O_2. Although the target concentration is very low, the signal can still be enlarged several times. So this method can be used to sensitively detection miRNA-155.

Please, insert Fig. 2 here.

3.4 Optimization of experimental conditions

To achieve optimal sensing performance, a time-course experiment was conducted and a certain volume of working solution of 10 mM PBS (pH 7.4) containing 1.0 mM H_2O_2 and 15 μL of 15 mM TMB. The amperometric response of the biosensor was detected in known concentrations of

miRNA-155. To obtain sufficient current, the influence of solution pH on the response was investigated as shown in Fig. 3A. In the examined pH range, the current reached maximum value at pH 7.4. In addition, HRP can noncovalently bind to the surface of GQDs through π-π interactions and electrostatic interactions. As anticipated, the current was enhanced rapidly with the increase of time with the RNA-155 concentration is 1 pM. As shown in Fig. 3B, after 60 min, the current signal approached a platform. Thus, 60 min was selected as the suitable incubated time between HRP and GQDs.

Please, insert Fig. 3 here.

3.5 Performance of the miRNA biosensor

Under the optimized conditions, different concentrations of miRNA-155 were analyzed by the sensor with amperometric detection in 10 mM pH 7.4 PBS. The amperometric responses of the biosensor to target miRNA at different concentrations under optimal experiment conditions are illustrated in Figure 4A. The electrochemical current increased with the increasing concentration of target RNA. As shown in Figure 4B, the amperometric current increased with the concentration of miRNA from 1 fM to 100 pM, and a liner relationship between current response and the logarithm of target miRNA concentrations was obtained in the insert picture. The linear equation was fitted as I (μA) = −0.8755−0. 1083lgc (pM) (R^2 = 0.9986) with a detection limit of 0.14 fM (S/N = 3).

Please, insert Fig. 4 here.

3.6 Selectivity, reproducibility and stability of the biosensor for miRNA detection

Sequence specificity in miRNAs detection is an important consideration because miRNA families often possess closely homologous sequences. To evaluate the specificity of the proposed method, several interfering agents were tested, including several bases mismatched strand (miRNA-21) and completely non-complementary DNA. The concentration of miRNA, DNA were 10 pM. As shown in

Fig. 5, two interfering agents produced two evidently signal decrease value, indicating that the fabricated biosensor owned high sequence specificity and excellent discrimination for similar miRNAs. Furthermore, five equally prepared electrodes showed acceptable reproducibility in response to 1 pM miRNA-155, the relative standard deviation (RSD) was 3.3%. In addition, after being stored for one week, the biosensor can still remain 85% of the initial response to 1 pM RNA, indicating the acceptable stability of the proposed biosensor. Good selectivity and stability of the biosensor can be attributed to the high surface to volume ratio of GQD and strong interaction between enzyme and GQD. The above results provided a simple immobilization procedure for sensitive detection of miRNA-155.

Please, insert Fig. 5 here.

3.7 Analytical application of the proposed biosensor

To further investigate the reliablity of the proposed biosensor, recovery experiments were performed by adding various concentration of miRNA-155 into the 10-fold diluted healthy human blood serum sample. Each sample was detected three times. The detection value was the average of three results. As tabulated in Table 1, the recovery and the RSD were ranging from 91.5% to 108% and from 1.5% to 2.5%, respectively, indicating that the biosensor was available for determining miRNA-155 in real biological samples.

Table 1. Determination of miRNA-155 added in human serum (n=3) with the biosensor

Serum sample	Added, pM	Found, nM	Recovery, %	RSD, %
1	0.001	0.001083	108	2.5
2	1	0.93	93	1.5
3	10	9.15	91.5	1.5

4. Conclusions

In summary, we developed a simple and sensitive electrochemical biosensor for covenient detection of miRNA-155 based on enzyme catalysis and GQDs as a new platform for immobilization. HRP can noncovalent assemble onto the surface of graphene quantum dots. Under the optimal conditions, the proposed method can sensitively detect miRNA-155 from 1 fM to 100 pM with a detection of 0.14 fM. Compared to some amplified detections for nucleic acids based on enzyme-assisted target recycling and carbon nanomaterial modified electrode, the proposed method has better stability and possesses a low detection limit and which is cheap and easy to operate, avoiding comlicated micro/nanofabrications. The proposed biosensor exhibited good selectivity and acceptable reproducibility for RNA detection and had a promising potential for RNA detection, providing a promising way for the determination of miRNA in clinical applications.

Acknowledgments

This work was supported by the National Natural Science Foundation of China (Nos.21175032, 21475032, 21405035), the Natural Science Fund for Creative Research Groups of Hubei Province of China (No.2014CFA015), and the Hubei Key Laboratory of Pollutant Analysis & Reuse Technology (No.KL2013M09).

Reference

Baker, S.N., Baker, G.A., 2010. Ange. Chem. Int. Edit. 49 (38), 6726-6744.

Causa, F., Aliberti, A., Cusano, A.M., Battista, E., Netti, P.A., 2015. J.Am. Chem. Soc. 137 (5), 1758-1761.

Cheng, F.F., He, T.T., Miao, H.T., Shi, J.J., Jiang, L.P., Zhu, J.J., 2015. ACS. Appl. Mater. Inter. 7 (4), 2979-2985.

Cheng, H., Zhao, Y., Fan, Y., Xie, X., Qu, L., Shi, G., 2012. ACS Nano 6 (3), 2237-2244.

Corsten, M.F., Papageorgiou, A., Verhesen, W., Carai, P., Lindow, M., Obad, S., Summer, G., Coort, S.L.M., Hazebroek, M., van Leeuwen, R., Gijbels, M.J.J., Wijnands, E., Biessen, E.A.L., De Winther, M.P.J., Stassen, F.R.M., Carmeliet, P., Kauppinen, S., Schroen, B., Heymans, S., 2012. Circ. Res. 111 (4), 415-425.

Ding, X., Yan, Y., Li, S., Zhang, Y., Cheng, W., Cheng, Q., Ding, S., 2015. Anal. Chim. Acta 874 (0), 59-65.

Duan, R., Zuo, X., Wang, S., Quan, X., Chen, D., Chen, Z., Jiang, L., Fan, C., Xia, F., 2013. J. Am. Chem. Soc. 135 (12), 4604-4607.

Ge, Z., Lin, M., Wang, P., Pei, H., Yan, J., Shi, J., Huang, Q., He, D., Fan, C., Zuo, X., 2014. Anal. Chem. 86 (4), 2124-2130.

Gupta, V., Chaudhary, N., Srivastava, R., Sharma, G.D., Bhardwaj, R., Chand, S., 2011. J. Am. Chem. Soc. 133 (26), 9960-9963.

Hao, N., Li, X.L., Zhang, H.R., Xu, J.J., Chen, H.Y., 2014. Chem. Commun. 50 (94), 14828-14830.

He, Y., Wang, X., Sun, J., Jiao, S., Chen, H., Gao, F., Wang, L., 2014. Anal. Chim. Acta 810, 71-78.

Jiang, C., Chen, X., Alattar, M., Wei, J., Liu, H., 2015. Cancer Gene Ther. 22 (6), 291-301.

Lewis, B.P., Shih, I.h., Jones-Rhoades, M.W., Bartel, D.P., Burge, C.B., 2003. Cell 115 (7), 787-798.

Li, L.L., Ji, J., Fei, R., Wang, C.Z., Lu, Q., Zhang, J.R., Jiang, L.P., Zhu, J.J., 2012. Adv. Funct. Mater. 22 (14), 2971-2979.

Li, L., Wu, G., Yang, G., Peng, J., Zhao, J., Zhu, J.J., 2013. Nanoscale 5 (10), 4015-4039.

Lim, L.P., Lau, N.C., Garrett-Engele, P., Grimson, A., Schelter, J.M., Castle, J., Bartel, D.P., Linsley, P.S., Johnson, J.M., 2005. Nature 433 (7027), 769-773.

Lin, L., Zhang, S., 2012. Chem. Commun. 48 (82), 10177-10179.

Liu, J., Lu, L., Li, A., Tang, J., Wang, S., Xu, S., Wang, L., 2015. Biosens. Bioelectron. 68 (0), 204-209.

Liu, Y., Dong, X., Chen, P., 2012. Chem. Soc. Rev. 41 (6), 2283-2307.

Lu, J., Getz, G., Miska, E.A., Alvarez-Saavedra, E., Lamb, J., Peck, D., Sweet-Cordero, A., Ebert, B.L., Mak, R.H., Ferrando, A.A., Downing, J.R., Jacks, T., Horvitz, H.R., Golub, T.R., 2005. Nature 435 (7043), 834-838.

Mitchell, P.S., Parkin, R.K., Kroh, E.M., Fritz, B.R., Wyman, S.K., Pogosova-Agadjanyan, E.L., Peterson, A., Noteboom, J., O'Briant, K.C., Allen, A., Lin, D.W., Urban, N., Drescher, C.W., Knudsen, B.S., Stirewalt, D.L., Gentleman, R., Vessella, R.L., Nelson, P.S., Martin, D.B., Tewari, M., 2008. P. Natl. Acad. Sci. 105 (30), 10513-10518.

O'Connell, R.M., Rao, D.S., Chaudhuri, A.A., Boldin, M.P., Taganov, K.D., Nicoll, J., Paquette, R.L., Baltimore, D., 2008. J. Exp. Med. 205 (3), 585-594.

O'Connell, R.M., Taganov, K.D., Boldin, M.P., Cheng, G., Baltimore, D., 2007. P. Natl. Acad. Sci. 104 (5), 1604-1609.

Pritchard, C.C., Cheng, H.H., Tewari, M., 2012. Nat. Rev. Genet. 13 (5), 358-369.

Qiu, X., Liu, X., Zhang, W., Zhang, H., Jiang, T., Fan, D., Luo, Y., 2015. Anal. Chem. 87 (12), 6303-6310.

Tang, L., Zeng, G., Shen, G., Li, Y., Liu, C., Li, Z., Luo, J., Fan, C., Yang, C., 2009. Biosens. Bioelectron. 24 (5), 1474-1479.

Wang, X., Chen, L., Su, X., Ai, S., 2013. Biosens. Bioelectron. 47 (0), 171-177.

Wang, X., Sun, X., He, H., Yang, H., Lao, J., Song, Y., Xia, Y., Xu, H., Zhang, X., Huang, F., 2015. J. Mater. Chem. B 3(17), 3583-3590.

Wang, X., Zhao, J., Huang, J., Tang, H., Yu, S., Chen, Y., 2012. Biochem. Bioph. Res. Co. 425 (1), 51-57.

Wei, L., Gong, X., Martinez, O.M., Krams, S.M., 2013. Transpl. Immunol. 29 (1–4), 123-129.

Wen, Y., Pei, H., Shen, Y., Xi, J., Lin, M., Lu, N., Shen, X., Li, J., Fan, C., 2012. Sci. Rep. 2.

Xiang, Q., Yu, J., Jaroniec, M., 2012. Chem. Soc. Rev. 41 (2), 782-796.

Yang, L., Liu, C., Ren, W., Li, Z., 2012. ACS. Appl. Mater. Inter. 4 (12), 6450-6453.

Zhang, P., Wu, X., Yuan, R., Chai, Y., 2015. Anal. Chem. 87 (6), 3202-3207.

Zhang, Y., Li, Z., Cheng, Y., Lv, X., 2009. Chem. Commun. (22), 3172-3174.

Zhu, S., Zhang, J., Liu, X., Li, B., Wang, X., Tang, S., Meng, Q., Li, Y., Shi, C., Hu, R., Yang, B., 2012. RSC. Adv. 2 (7), 2717-2720.

Zhu, Y., Murali, S., Cai, W., Li, X., Suk, J.W., Potts, J.R., Ruoff, R.S., 2010. Adv. Mater. 22 (35), 3906-3924.

Highlights

1. Graphene quantum dots (GQDs) were used as a new substrate for HRP immobilization.
2. We developed a electrochemical biosensor based on horseradish peroxidase (HRP)-assisted catalytic reaction for sensitive detection of miRNA-155.
3. The method has been applied in human serum, with good selectivity and good recovery.

Graphical abstract

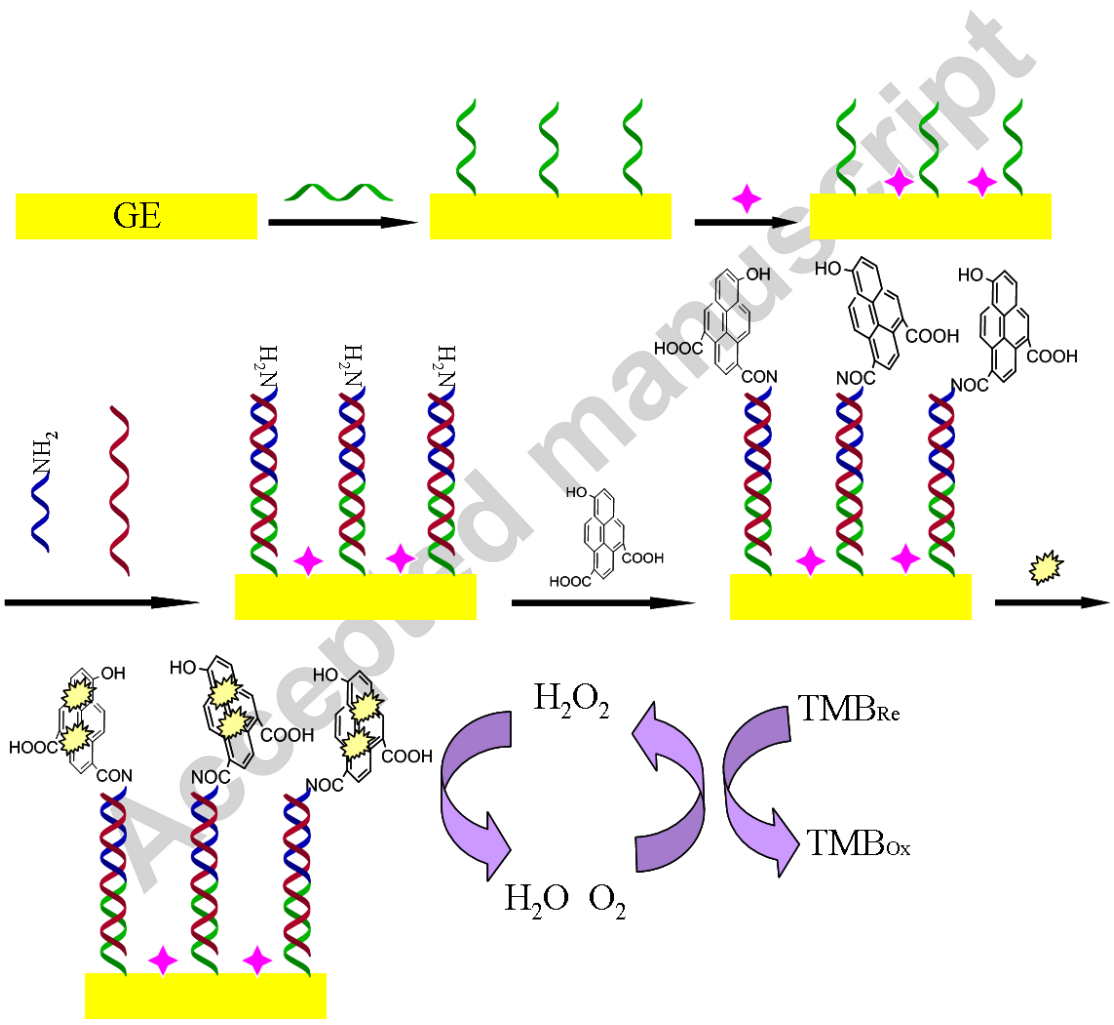

Figures

Figure 1. Principle of the enzyme catalytic amplification of miRNA-155 detection with graphene quantum dot-based electrochemical biosensor

Figure 2. Amperometric responses of the electrochemical biosensor after 60 min incubation with: no target (a), no HRP (b), HRP (c). The amperometric detection was conducted in 10 mM PBS (pH 7.4) containing 1.0 mM H_2O_2 and 15 μL of 15 mM TMB.

Figure 3. Effects of (A) pH value of buffer solution in RNA sensor, the miRNA-155 concentration is 10 fM, (B) noncovalent assembly time between GQDs and HRP, the miRNA-155 concentration is 1 pM.

Figure 4. Current responses of 0.001, 0.01, 0.1, 1, 10, 100 pM miRNA-155 in PBS (7.4) (a), relationship between current and RNA concentration. The insert showed the linear relationship between the current and the concentration of miRNA-155 (b). The error bars represent the standard deviation of three measurements.

Figure 5. Selectivity of the proposed electrochemical biosensor to miRNA-21, DNA at 10 pM, respectively. The concentration of miRNA-155 is 1 pM. Error bars are obtained based on three independent measurements.

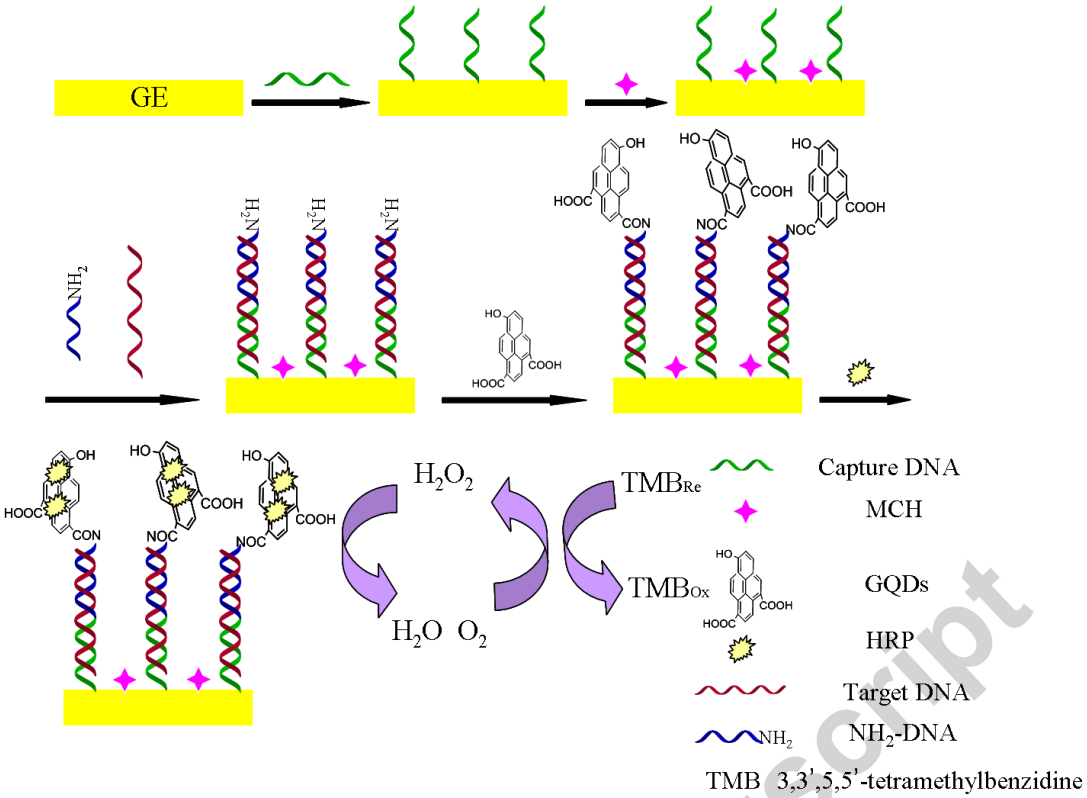

Fig. 1

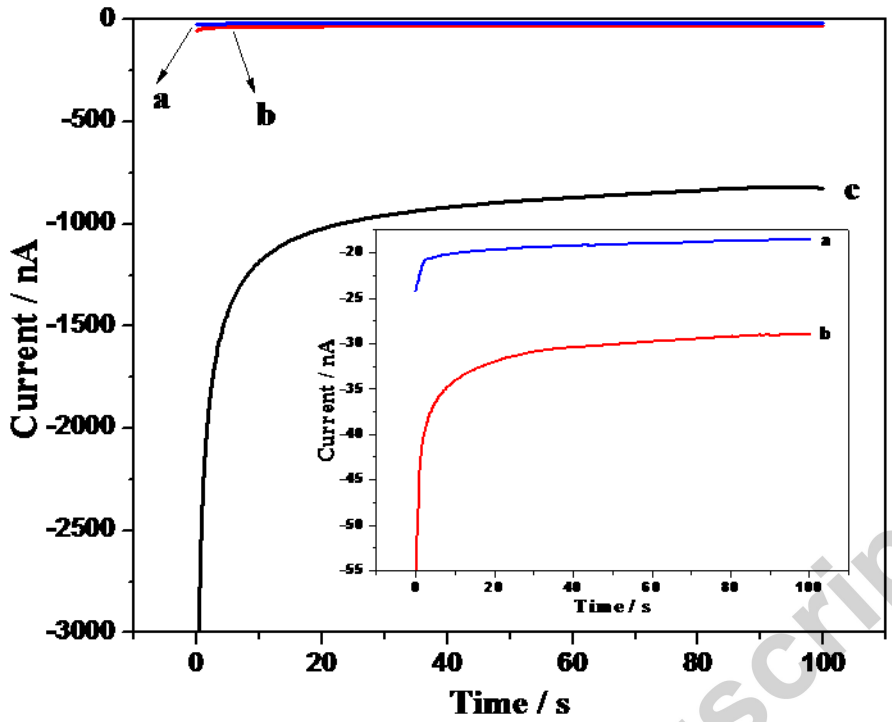

Fig. 2

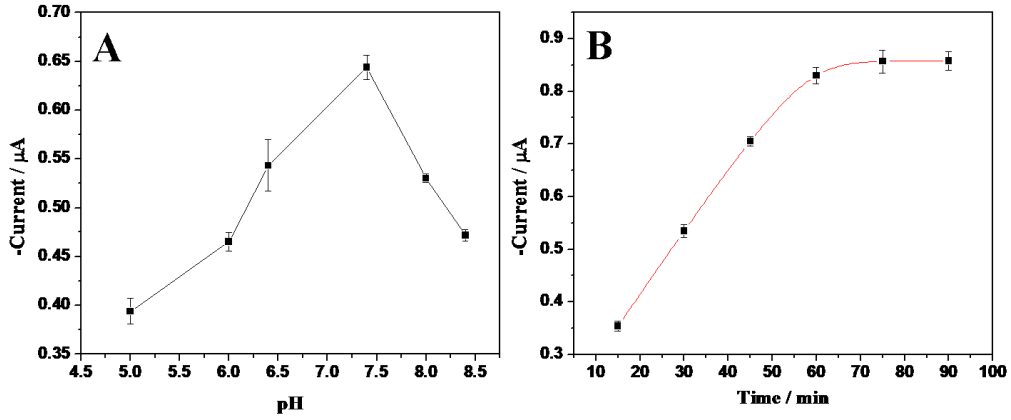

Fig. 3

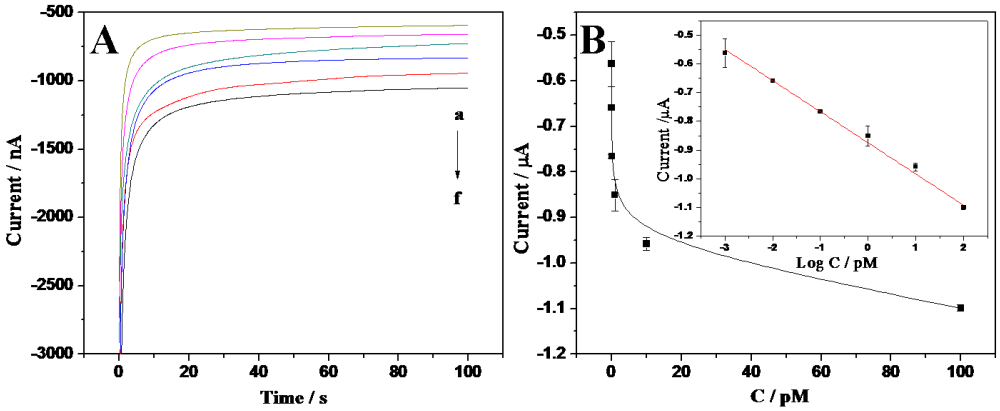

Fig. 4

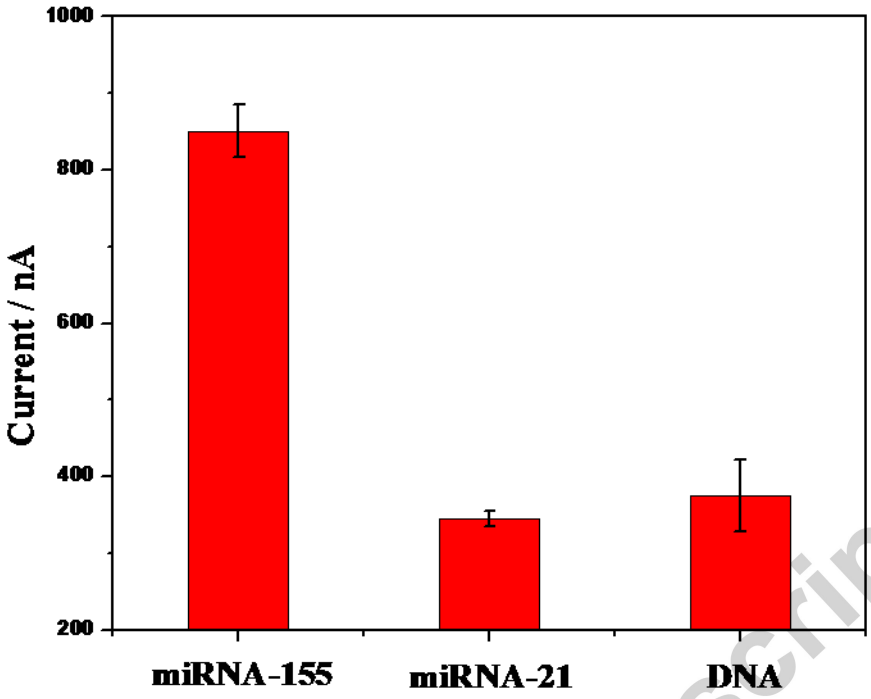

Fig. 5